

Near-Infrared Light Photovoltaic Detector Based on GaAs Nanocone Array/Monolayer Graphene Schottky Junction

Lin-Bao Luo,* Jing-Jing Chen, Ming-Zheng Wang, Han Hu, Chun-Yan Wu, Qiang Li, Li Wang, Jian-An Huang,* and Feng-Xia Liang*

Near infrared light photodiodes have been attracting increasing research interest due to their wide application in various fields. In this study, the fabrication of a new *n*-type GaAs nanocone (GaAsNCs) array/monolayer graphene (MLG) Schottky junction is reported for NIR light detection. The NIR photodetector (NIRPD) shows obvious rectifying behavior with a turn-on voltage of 0.6 V. Further device analysis reveals that the photovoltaic NIRPDs are highly sensitive to 850 nm light illumination, with a fast response speed and good spectral selectivity at zero bias voltage. It is also revealed that the NIRPD is capable of monitoring high-switching frequency optical signals (~2000 Hz) with a high relative balance. Theoretical simulations based on finite difference time domain (FDTD) analysis finds that the high device performance is partially associated with the optical property, which can trap most incident photons in an efficient way. It is expected that such a self-driven NIRPD will have potential application in future optoelectronic devices.

further serve these applications. Compared with the conventional IRPDs (e.g., quantum dot IRPDs,^[6] quantum well IRPDs,^[7] strained layer superlattice IRPDs,^[8] and bulk IRPDs^[9]), photoconductor and photodiode IRPDs are two kinds of devices that have garnered special interest owing to their high performance and simple structures. Photoconductor IRPDs normally exhibit unparalleled performance in terms of high responsivity (R) and high photoconductive gain (G), whereas photodiode IRPDs have advantages in sensitivity and response speed.^[10,11] In addition, photovoltaic behavior can be observed in photodiode-based devices. This feature renders it possible to detect light irradiation without an exterior power supply.^[7,12]

1. Introduction

Infrared light, as electromagnetic radiation with longer wavelengths than visible light, has been widely used in thermal efficiency analysis, remote temperature sensing, and environmental monitoring.^[1,2] In addition to these non-military purposes, IR has been extensively used for military applications including target acquisition, surveillance, and night vision.^[3–5] As such, researchers have invested tremendous time and effort into developing new IR photodetector (IRPD) technologies to

Gallium arsenide (GaAs), with a direct bandgap of ~1.42 eV, is a promising material for optoelectronic device applications. Due to enhanced optical properties, lower cost, and a greater energy-conversion efficiency compared to conventional thin-film devices, photovoltaic devices employing large-areas and lithographically defined vertical arrays of 1D GaAs nanostructures such as nanowires (NWs)^[13,14] and nanopillars (NPs)^[15,16] have attracted extensive attention in the past decade. In spite of the tremendous progress in photovoltaic device applications, the exploration of 1D GaAs nanostructure arrays as photosensors for IR detection has been seldom studied.^[17] In this work, we present the fabrication of new Schottky junction NIRPDs by coating GaAs nanocone (GaAsNC) arrays with monolayer graphene (MLG), a single-atomic macromolecule with high mobility, conductivity, and flexibility, as well as perfect light transparency that has been successfully combined with other semiconductor materials such as Si or CdSe for high-performance photodetector applications.^[18,19] As observed in ZnONCs and SiNCs,^[20,21] the GaAsNC array is capable of trapping incident light with the nanostructures, which is highly beneficial to photodetection. Electrical analysis reveals that NIR photodetectors exhibit obvious rectification behavior with a turn-on voltage of 0.6 V, and photovoltaic characteristics with an open-circuit voltage (V_{OC}), a short-circuit current (I_{SC}), and a fill factor (FF) of 0.15 V, 4.1 μ A, and 0.19, respectively, under light illumination. It is also observed that NIRPD is highly sensitive to NIR light illumination with good selectivity and a fast response speed. Further finite difference time domain (FDTD) modeling of the GaAsNC array reveals that the incident NIR light can be

Prof. L.-B. Luo, J.-J. Chen, M.-Z. Wang, H. Hu, Dr. C.-Y. Wu, Dr. Q. Li, Dr. L. Wang
School of Electronic Science and Applied Physics
and Anhui Provincial Key Laboratory
of Advanced Functional Materials and Devices
Hefei University of Technology
Hefei, Anhui, 230009, PR China
E-mail: luolb@hfut.edu.cn



Dr. J.-A. Huang
Center of Super-Diamond and Advanced Films (COSDAF)
and Department of Physics and Materials Science
City University of Hong Kong
Hong Kong SAR, PR China
E-mail: vjahuang2-c@my.cityu.edu.hk

Dr. F.-X. Liang
School of Materials Science and Engineering
Hefei University of Technology
Hefei, Anhui, 230009, PR China
E-mail: fxliang@hfut.edu.cn

DOI: 10.1002/adfm.201303368

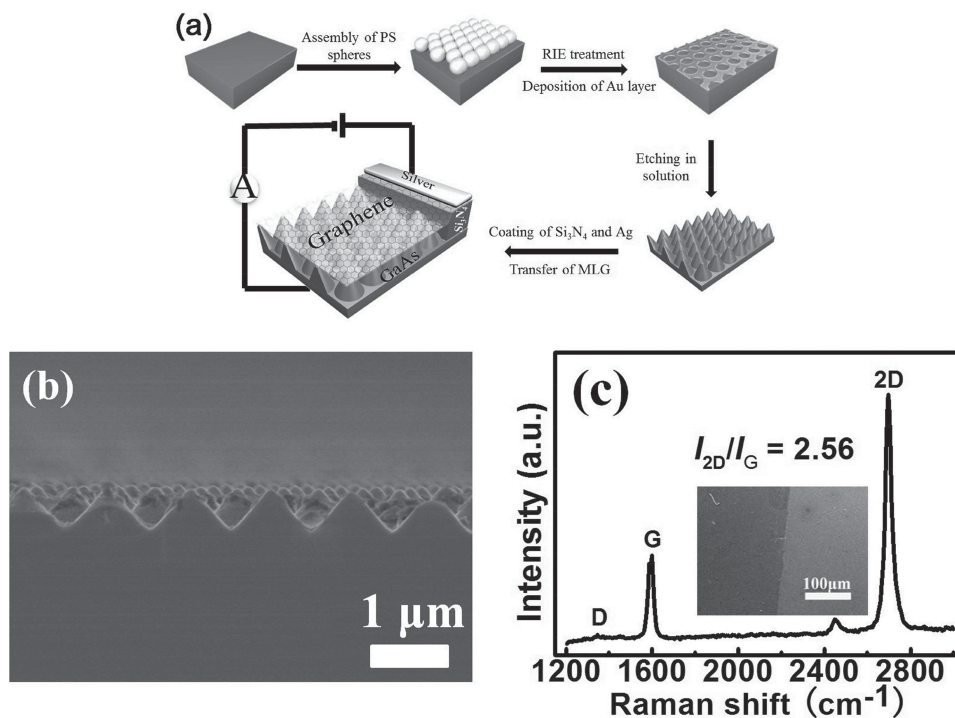


Figure 1. a) Schematic illustration of the device fabrication process. b) A typical cross-sectional scanning electron microscope (SEM) image of the *n*-GaAsNCs array after etching. c) Raman spectrum of the MLG layer.

trapped within the NC array or above the GaAsNC/MLG contact, consistent with the observed excellent device performance.

2. Results and Discussion

The scheme in **Figure 1a** elaborates the detailed procedures to construct the GaAsNC array/MLG Schottky junction NIRPDs. First, a highly ordered hexagonal-packed monolayer of polystyrene (PS) spheres was allowed to self-assemble on an *n*-type GaAs substrate by a slow-pulling strategy.^[22] The close-packed monolayer assembly was then transformed into a non-close-packed arrangement by reactive ion etching (RIE) treatment, after which a 20 nm thick gold film was deposited via electron beam evaporator. The PS spheres were then lifted off to expose Au film with a hexagonal array of holes which can direct the chemical etching of the GaAs in a mixture of deionized water, H₂SO₄, and K₂Cr₂O₇,^[23] as in the fabrication of SiNWs.^[24] Due to the isotropic etching of GaAs in etchant solution, the nanostructures obtained via this method is GaAsNC array with a diameter and height of 1 μm and 500 nm, respectively, (cf. **Figure 1b**). To assemble the device, the as-etched GaAsNC array was then coated with a layer of Si₃N₄ thin-film on one side, followed by transfer of the MLG film onto the surface of the GaAsNC array. A Raman spectroscopy study of the graphene

shows two strong peaks: a 2D peak (2698 cm⁻¹) and a G peak (1600 cm⁻¹), with an intensity ratio of ≈2.56, indicative of the high quality of the MLG film. The negligible D peak observed at 1346 cm⁻¹ signifies a low amount of defects.

Figure 2a shows a typical room-temperature *I*-*V* curve of the *n*-GaAsNC array/MLG junction in the dark, from which we can see obvious rectification behavior. In view of the fact that silver can form good contact (Ohmic contact) to MLG, and Ag-Sn is also a good electrode for *n*-GaAs, the observed rectifying effect can be exclusively ascribed to the *n*-GaAsNC array/MLG junction. The turn-on voltage is deduced to be 0.6 V, comparable to that of CdSe nanoribbon/MLG^[19] and ZnO/MLG heterojunctions.^[25] Moreover, the on-off ratio is determined to be

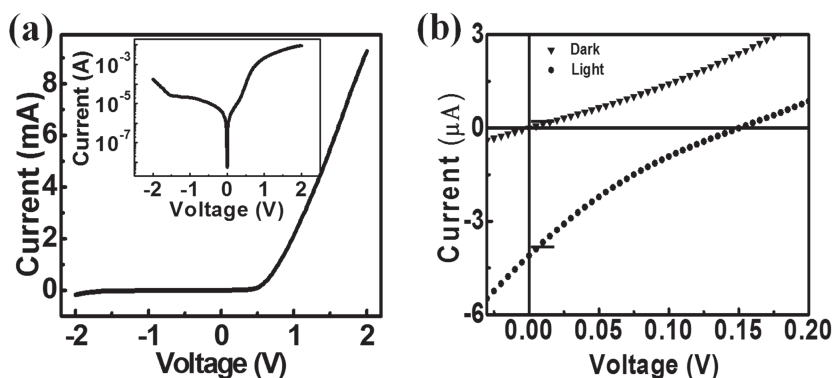


Figure 2. a) Typical *I*-*V* characteristics of the Schottky junction measured at ambient condition in the dark. b) *I*-*V* characteristics of the GaAsNC array/MLG Schottky junction under illumination of 850 nm light. During measurement, the light intensity was kept at 5 mW cm⁻².

10^2 (from -1 to 1 V). Such a low value is associated with the low Schottky barrier height of the n -GaAsNC array/MLG Schottky junction, which can be described by the thermionic emission-based diode equation:^[26]

$$J(T, V) = J_s(T) \left[\exp\left(\frac{eV}{nK_B T}\right) - 1 \right] \quad (1)$$

where $J(T, V)$ is the current density across the GaAs nanocone array/MLG interface, V is the applied voltage, k_B is the Boltzmann constant, T is the temperature, and n the ideality factor ($n = (q/kT)(dV/d \ln I)$). The prefactor, $J_s(T)$, is the saturation current density and is expressed by $J_s(T) = A^* T^2 \exp(-e\phi_{SBH}/K_B T)$, where ϕ_{SBH} is the zero-bias Schottky barrier height (SBH), A^* the Richardson constant ($A^* = 4\pi q m^* k^2/h^3$), and m^* the effective mass of the charge carriers. For GaAs, A^* is theoretically estimated to be $7.56 \text{ A cm}^{-2} \text{ K}^{-2}$ ($m_e^* = 0.063 m_0$), and the ideality factor n is determined to be 3.25. Using the J_s value, the Schottky barrier height at the n -GaAsNC array/MLG interface (ϕ_{SBH}) was estimated to be 0.71 V. In addition, when illuminated with 850 nm light (5 mW cm^{-2}), the n -GaAsNC array/MLG junction exhibits apparent photovoltaic behavior, with an open-circuit voltage (V_{OC}), a short-circuit current (I_{SC}), and a fill factor (FF) of 0.15 V, 4.1 μA , and 0.19, respectively, as shown in Figure 2b. Though the energy conversion efficiency is very low (less than 0.1%), the heterojunction can enable detection of NIR without an external power supply.

To further study the photosensitivity of the Schottky junction photodetector, the photoresponse characteristics under light illumination of different intensities were investigated. As observed from Figure 3a, the photocurrent increases sharply and is stabilized at an 'On' state upon light irradiation, but it decrease quickly to an 'Off' state when the light was turned off, leading to a on-off ratio as high as 10^4 . It is also observed that the photocurrent increases almost linearly with the light intensity (see the inset of Figure 3). Further quantitative analysis of the relationship between photocurrent and light intensity reveals that the photocurrent can be fitted with a simple power law, $I = AP^\theta$, where A is a constant for a certain wavelength, P is the power of illumination, and the exponent θ determines the response of photocurrent to light intensity.^[27] Fitting the equation to the experimental data gives $\theta = 0.97$. Such a large θ value (very close to 1) for our photodetector suggests that a low amount of trap states are present in the GaAsNC array after surface passivation.

Based on Figure 3, we next calculate the responsivity (R) and detectivity (D^*), two favored metrics that are normally used to delineate NIRPD performance, so as to evaluate the

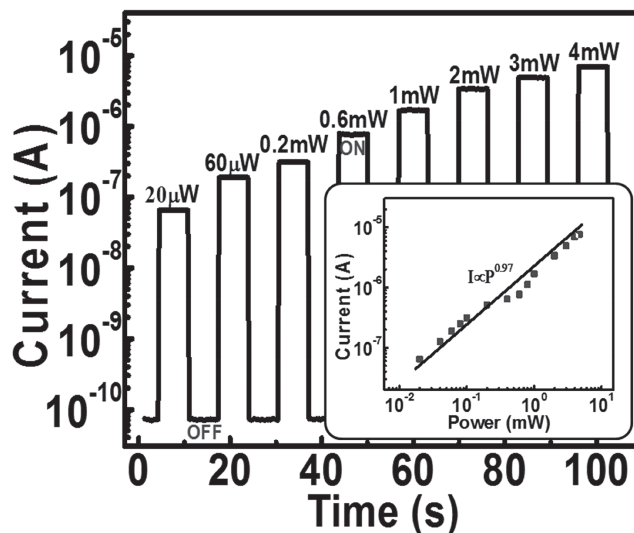


Figure 3. a) Photoresponse of the NIRPD under various light intensities. b) The fitting of the relationship between the photocurrent and light intensity.

device performance in a more quantitative way. For the present n -GaAsNC array/MLG junction NIRPD, the two parameters can be described as^[28]

$$R(\text{A W}^{-1}) = \frac{I_p - I_d}{P_{opt}} \quad (2)$$

$$D^* = \sqrt{\frac{A}{2qI_d}} R \quad (3)$$

where I_p is the photocurrent, P_{opt} is the incident light power, η is the quantum efficiency, h is Planck's constant, c is light speed, λ is the incident light wavelength, A is the area of the n -GaAsNC array/MLG junction NIRPD (0.25 cm^2), q is the charge of an electron, and I_d is the dark current. Based on these values, R and D^* are estimated to be 3.73 mA W^{-1} and $1.83 \times 10^{11} \text{ cm Hz}^{1/2} \text{ W}^{-1}$ at zero bias, respectively. **Table 1** summarizes the key metrics of other NIRPDs. One can see that, though the responsivity of the present device is inferior to other devices, other major parameters in terms of the response speed (τ_r/τ_f), on-off ratio (I_{light}/I_{dark}), and detectivity (D^*) are considerably improved, suggesting the great potential of our device for future NIRPD applications.

Table 1. Comparison of the device performance of the current GaAsNC/MLG array Schottky junction with other NIRPDs.

Device Structure	Responsivity	τ_r/τ_f	I_{light}/I_{dark}	detectivity	Ref
GaAsNC/MLG array Schottky junction	1.73 mA/W	72/122 μs	10^4	1.83×10^{11}	This work
Pd/CNT/Sc barrier free bipolar diode	98.7 $\mu\text{A/W}$	~	~	1.09×10^7	29
InAs/GaAs QD heterojunction	2 mA/W	~	~	2.94×10^9	30
Si/MLG heterojunction	225 mA/W	1.2/3 ms	10^4	7.69×10^9	20
CdTe nanoribbons based NIRPD	$7.8 \times 10^2 \text{ A/W}$	1.1/20.4 s	1.1	~	31

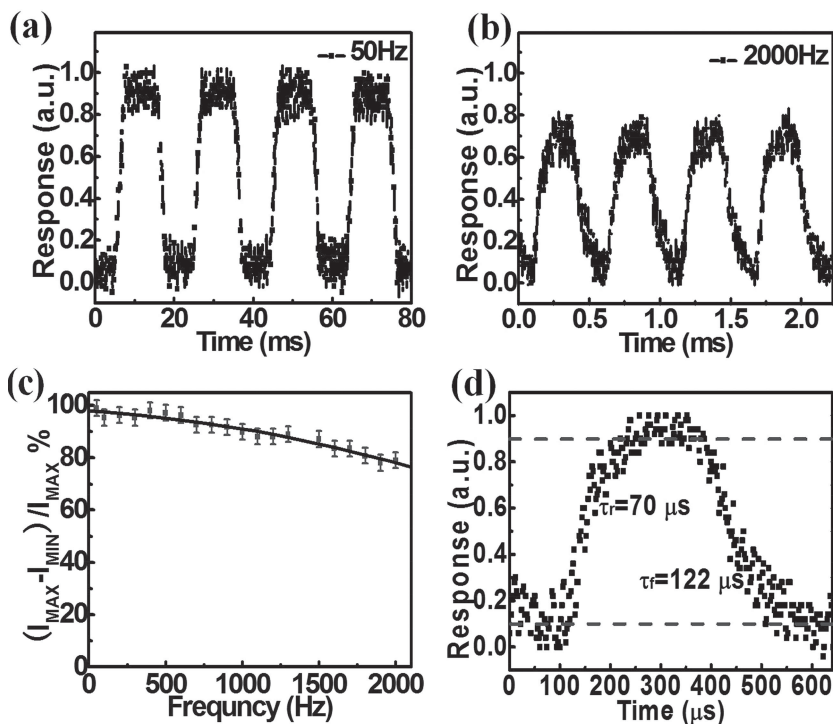


Figure 4. Response of the Schottky junction to pulsed NIR light at a frequency of a) 50 or b) 2000 Hz. c) The relative balance versus switching frequency of the optical chopper. d) A single normalized cycle at 50 Hz to estimate both rise time (τ_r) and fall time (τ_f).

To explore the feasibility of the current device for practical applications in optical communications and optical switches, the response speed of the *n*-GaAsNC array/MLG junction photodetector was further studied by using an oscilloscope to monitor the variation of the photocurrent under pulsed light, which was generated by a mechanical chopper. We find that our device could work over a wide frequency range, from 50 to 2000 Hz, under 850 nm light illumination with a fixed intensity of 5 mW cm^{-2} , with excellent stability and reproducibility (Figure 4a,b). In particular, even at 2000 Hz, the $[I_{\text{max}} - I_{\text{min}}]/I_{\text{max}}$ value only decreases by $\sim 20\%$ (Figure 4c), which means that our device is capable of monitoring pulsed light with a very high switching frequency. Generally, the speed of a photodetector is often evaluated by the rise time (τ_r) and the fall time (τ_f) of its response to an pulsed signal.^[32] Careful analysis of the *n*-GaAsNC array/MLG Schottky junction device reveals a small τ_r of 72 μs and a small τ_f of 122 μs (Figure 4d). These values are much faster than the reported Si/MLG heterojunction and CdTe nanowire-based NIRPDs.^[20,31] Understandably, such a fast response speed could be associated with the Schottky junction formed between the MLG and the *n*-GaAsNC array, which can facilitate the effective and rapid separation of the photogenerated carriers.^[33]

In addition to the rapid photoresponse, our device exhibits excellent spectral selectivity as well. Figure 5a depicts the spectral response of the Schottky junction device to light illumination with wavelengths ranging from 650 to 1050 nm. One can see that the NIRPD shows the highest sensitivity to 850 nm

light, whereas it is nearly blind to lower wavelengths. This spectral sensitivity is reasonably associated with the working mechanism of the device shown in Figure 5b. A built-in potential in GaAs near the interface (the depletion region) was formed due to the difference in work functions between the graphene and GaAs. When irradiated, the photogenerated holes (h^+) and electrons (e^-) in the depletion region can be extracted by the electric field. What is more, the minority carriers (holes) generated within a diffusion length from the depletion region can diffuse to the depletion region. Both process can contribute to the photocurrent in the circuit. Remarkably, this process is not spontaneous, as the photogeneration of carriers can happen only on the condition that the energy of the incident photons is larger than the bandgap of GaAs (1.42 eV, $\sim 870 \text{ nm}$).

To unveil the underlying reasons for the high performance of the NIRPD, we examined the optical properties of *n*-GaAsNC array/MLG junction by using FDTD. Figure 6 shows the simulated distributions of electric field intensity when irradiated by wavelengths of 650, 720, 870, and 1040 nm. Interestingly, it can

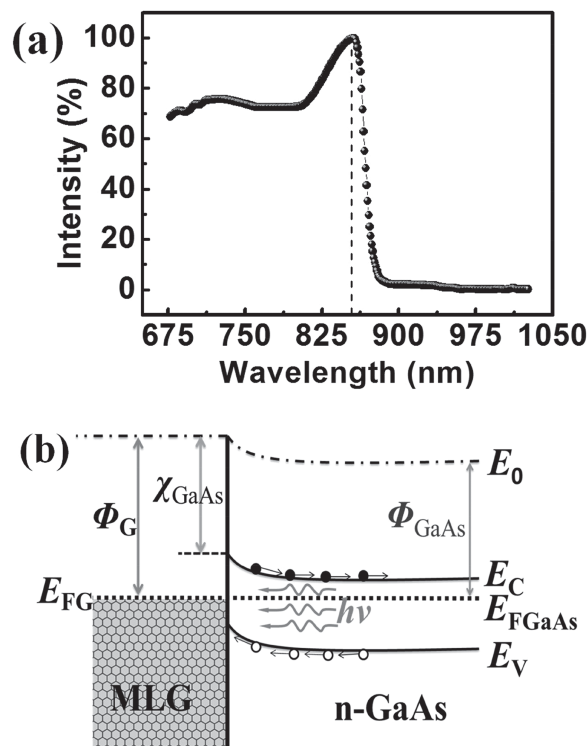


Figure 5. a) Spectral response of the NIRPD, during the spectral response study, the light intensities were kept at the same value. b) Energy band diagram of the NIRPD upon light illumination.

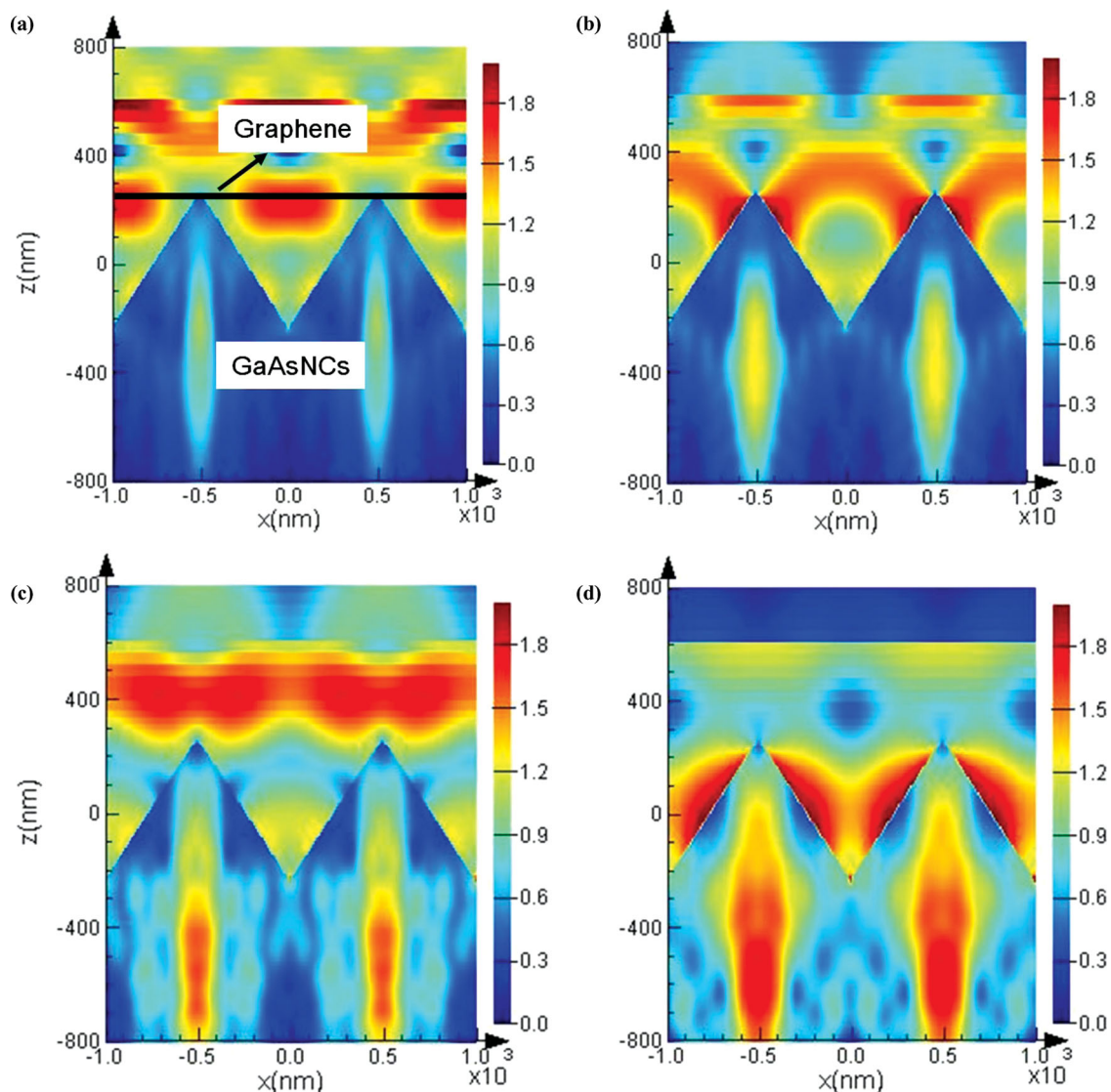


Figure 6. Simulated electric field energy density distribution of the *n*-GaAsNC array/MLG under light illumination with intensities of 650 nm (a), 720 nm (b), 870 nm (c), and 1040 nm (d).

be seen that the electric field energy-density distribution is highly dependent on the wavelength of incident light: for 650 nm irradiation, there is no obvious electric field within the nanostructures (Figure 6a). When the wavelength was increased to 720 nm, a weak electric field at the lower part of the nanocone and a strong electric field close to the GaAsNC/MLG contact were observed. As the wavelength was further increased to 870 nm, the enhanced electric field changes substantially, giving rise to two strong electric fields (one at the lower part inside the nanocone, and another one at the tip). This finding is totally different from the electric field distribution of graphene on GaAs wafers under identical simulation conditions in **Figure 7**, showing that the fields were typical plane wave profiles, which is the same as the incident light, and no optical resonances could be

found at the wavelengths of 650, 720, 870, or 1040 nm. This special optical property known as resonant absorption^[34,35] and nanofocusing^[36,37] is highly beneficial to NIR detection. The incident light at 870 nm is resonant with the nanocone structures such that enhanced energy is efficiently trapped at the bottom in the nanocones, which would be eventually absorbed to generate carriers. Nanofocusing, on the other hand, confines photons at the tip where the graphene is in contact with the NCs, which will lead to a very high energy-utilization efficiency. It should be noted that, though the present NCs are able to trap 1040 nm light in a more efficient way (Figure 6d), they can hardly sense this light illumination as the energy of the incident photons is insufficient to lift electrons directly from the valence band to the conduction band in the GaAsNCs.

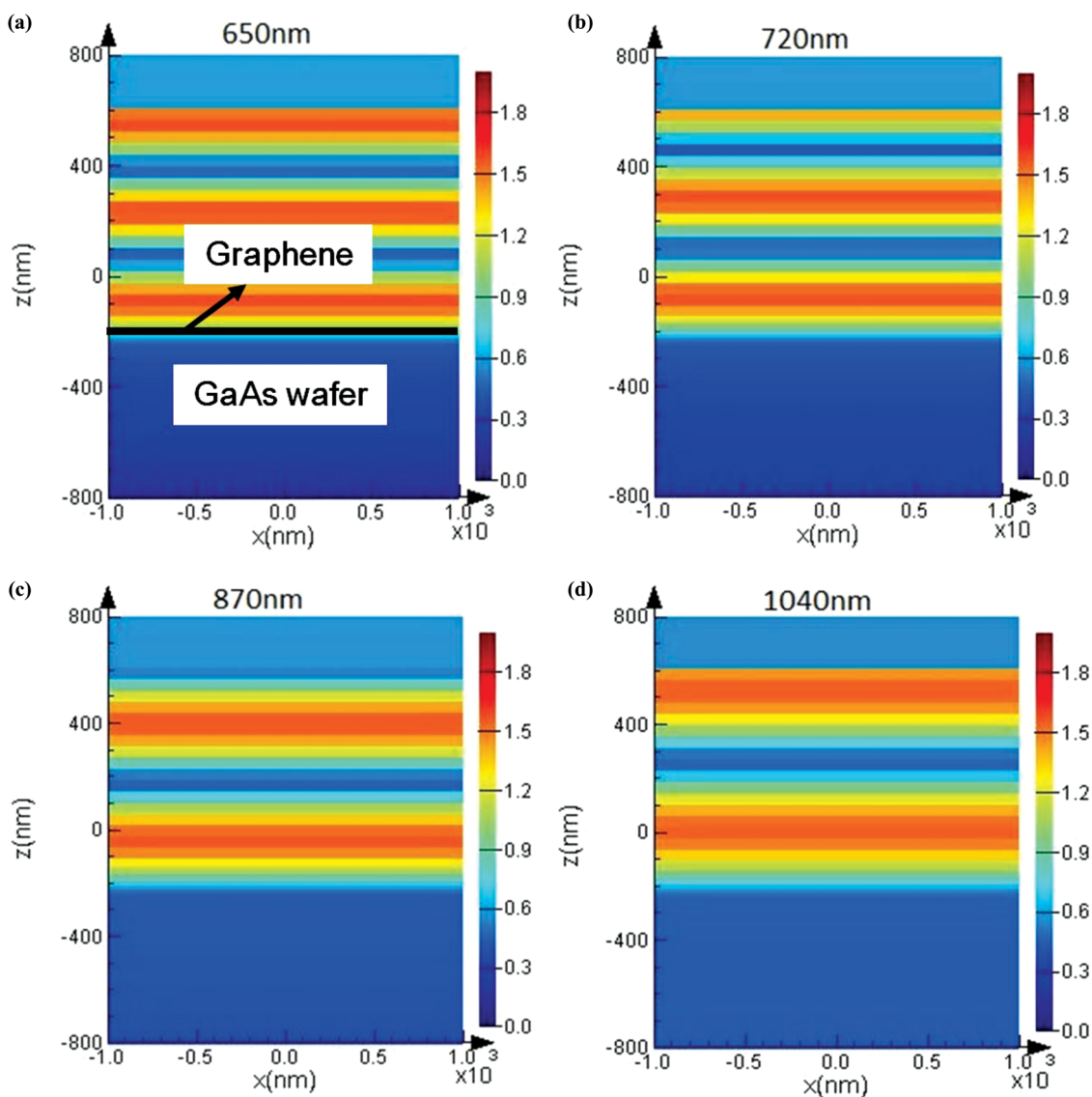


Figure 7. Simulated electric field energy density distribution of the GaAs wafer/MLG under light illumination with intensities of 650 nm (a), 720 nm (b), 870 nm (c), and 1040 nm (d).

3. Conclusion

We demonstrate a high-performance NIRPD by simply coating *n*-GaAsNC array with a layer of high-quality MLG. Device performance analysis reveals that the NIRPD exhibits high sensitivity to 850 nm illumination under zero bias with a fast response speed ($\tau_r = 72 \mu\text{s}$, $\tau_f = 122 \mu\text{s}$), excellent selectivity, and good reproducibility in a wide range of switching frequencies (50–2000 Hz). What is more, the on–off ratio, responsivity, and detectivity of the device were estimated to be 10^4 , 1.73 mA W^{-1} and $1.83 \times 10^{11} \text{ cm Hz}^{1/2} \text{ W}^{-1}$, higher than other NIRPDs. Theoretical simulation of the GaAsNC array based on FDTD reveals that the incident NIR light can be trapped within the NC array, consistent with the observed excellent device performance. This study suggests that our *n*-GaAsNC array/MLG Schottky junction NIRPDs will have potential application in future optoelectronic devices.

4. Experimental Section

Synthesis and Characterization of MLG Film and GaAsNC Array: The monolayer graphene (MLG) films were fabricated through a chemical vapor deposition (CVD) method at 1000 °C using a mixed gas of CH_4 (40 standard cubic centimeter per minute (SCCM)) and H_2 (20 SCCM) as reaction source. After deposition, the graphene films deposited on 25 μm thick Cu foils were spin-coated with polymethylmethacrylate (PMMA) solution (5 wt% in chlorobenzene) and the Cu substrates were etched away in Marble's reagent solution. The GaAsNC array was synthesized via a metal-assisted chemical etching approach. *n*-type GaAs wafer was ultrasonicated in acetone and ethanol at room temperature for 10 and 5 min, respectively, to remove contamination or organic grease. Then, the native-oxide film was removed by briefly dipping the substrate into an aqueous HF solution (46 wt%), followed by rinsing with deionized water for several times. The cleaned GaAs wafer was next cut into 2 cm \times 2 cm pieces on which monolayers PS spheres with diameters of $\sim 960 \text{ nm}$ were assembled by a modified drop-coating technique. The close-packed monolayer PS was transformed into a non-close-packed

arrangement by reactive ion etching (RIE) treatment. The flow gas in the RIE experiments was oxygen at a flow rate of 20 SCCM and a pressure of 3 Pa, and the applied RF power was 50 W. Afterwards, a 20 nm thick Au layer was evaporated on the GaAs surface. For the solution etching process, an etching mixture composed of deionized water, $K_2Cr_2O_7$, H_2SO_4 was used at room temperature. The concentrations of $K_2Cr_2O_7$ and H_2SO_4 were 3 and 1 M, respectively. After etching, the substrate was immersed in CH_3COCH_3 for 30 min to remove the PS spheres. The Au film was removed by immersing in the solution of I_2/KI for 15 min. The Raman analysis of the MLG was performed on a Raman spectrum (JY, LabRAM HR800), the morphologies of the GaAsNC array was examined by field-emission scanning electron microscopy (FESEM, SIRION 200 FEG).

Device Fabrication and Characterization: To fabricate *n*-GaAsNC array/MLG NIRPDs, GaAsNC array was immersed in an aqueous hydrochloric acid (HCl, 10% (v/v)) solution for 45 s to remove possible native oxide on the surface, followed by chemical passivation by means of ammonium sulfide $[(NH_4)_2S]$ solution (22% (v/v)) for 90 min to minimize the surface-state density. After that, Si_3N_4 thin-film was deposited on one side of the GaAs nanocone array. Then, MLG film was transferred onto the surface of the GaAsNC array. Finally, Ag–Sn was deposited on the rear side of GaAs, and Ag paste was placed at the corners of the MLG films where the Si_3N_4 film was deposited. The electrical characteristics of the Schottky junction NIRPDs were measured using a semiconductor characterization system (Keithley 4200-SCS). To study the optoelectronic properties, incident lights from both xenon lamp (5 mW cm^{-2}) and a monochromator (Omni-1300) were perpendicularly focused and guided onto the NIRPDs.

Theoretical Simulation: The simulation was done by the Lumerical FDTD Solutions. The model is composed of two GaAs nancones on a GaAs wafer with a bottom radius of 500 nm and height of 500 nm. The MLG with 1 nm thickness was placed on top of the GaAs nanocones. The dielectric constant of undoped MLG was 2.5 according to W. Gao et al.^[39] The optical data of GaAs was obtained from Palik.^[38] The illumination was plane wave of wavelength 600–1100 nm with polarization parallel to the axis between two cones. The boundary conditions at *x*, *y* were periodic and perfect matching layer (PML) at *z*. One monitor was placed 600 nm above of the nanocones for reflectance and another at the cross-section plane between two cones for distribution of electric field intensity.

Acknowledgements

This work was supported by the National Natural Science Foundation of China (NSFC, Nos. 51172151, 21101051), the Fundamental Research Funds for the Central Universities (2011HGZJ0004, 2012HGXC0003, 2013HGCH0012), the China Postdoctoral Science Foundation (103471013).

Received: September 30, 2013

Revised: November 18, 2013

Published online: January 21, 2014

- [1] J. F. Wang, M. S. Gudiksen, X. F. Duan, Y. Cui, C. M. Lieber, *Science* **2001**, 293, 1455.
- [2] Q. L. Bao, K. P. Loh, *ACS Nano* **2012**, 6, 3677.
- [3] C. Downs, T. E. Vandervelde, *Sensors* **2013**, 13, 5054.
- [4] C. Li, Y. Bando, M. Y. Liao, Y. Koide, D. Golberg, *Appl. Phys. Lett.* **2010**, 97, 161102.
- [5] P. C. Wu, Y. Dai, Y. Ye, Y. Yin, L. Dai, *J. Mater. Chem.* **2011**, 21, 2563.
- [6] A. I. Yakimov, A. V. Dvurechenskii, A. I. Nikiforov, Y. Y. Proskuryakov, *Appl. Phys. Lett.* **2001**, 89, 5676.

- [7] J. Tatebayashi, A. Jallipalli, M. N. Kutty, S. H. Huang, T. J. Rotter, G. Balakrishnan, L. R. Dawson, D. L. Huffaker, *J. Electron. Mater.* **2008**, 37, 1758.
- [8] G. E. Bulman, D. R. Myers, J. J. Wiczer, L. R. Dawson, R. M. Biefeld, T. E. Zipperian, *IEEE Electron. Devices Meet.* **1984**, 30, 719.
- [9] V. V. Vasilyev, V. N. Ovsyuk, Y. G. Sidorov, *Proc. SPIE* **2003**, 5065, 39.
- [10] D. Wu, Y. Jiang, Y. G. Zhang, J. Li, Y. Q. Yu, Y. Zhang, Z. F. Zhu, L. Wang, C. Y. Wu, L. B. Luo, *J. Mater. Chem.* **2012**, 22, 6206.
- [11] C. W. Liang, S. Roth, *Nano Lett.* **2008**, 8, 1809.
- [12] J. J. Hassan, M. A. Mahdi, S. J. Kasim, N. M. Ahmed, H. Abu Hassan, Z. Hassan, *Appl. Phys. Lett.* **2012**, 101, 261108.
- [13] J. A. Czaban, D. A. Thompson, R. R. LaPierre, *Nano Lett.* **2008**, 8, 148.
- [14] B. Hua, J. Motohisa, Y. Kobayashi, S. Hara, T. Fukui, *Nano Lett.* **2009**, 9, 112.
- [15] P. Senanayake, C. H. Hung, J. Shapiro, A. Lin, B. Liang, B. S. Williams, D. L. Huffaker, *Nano Lett.* **2011**, 11, 5279.
- [16] G. Mariani, R. B. Laghumavarapu, B. T. de Villiers, J. Shapiro, P. Senanayake, A. Lin, B. J. Schwartz, D. L. Huffaker, *Appl. Phys. Lett.* **2010**, 97, 013107.
- [17] P. Senanayake, C. H. Hung, J. Shapiro, A. Lin, B. L. Liang, B. S. Williams, D. L. Huffaker, *Nano Lett.* **2011**, 11, 5279.
- [18] X. H. An, F. Z. Liu, Y. J. Jung, S. Kar, *Nano Lett.* **2013**, 13, 909.
- [19] Z. W. Gao, W. F. Jin, Y. Zhou, Y. Dai, B. Yu, C. Liu, W. J. Xu, Y. P. Li, H. L. Peng, Z. F. Liu, *Nanoscale* **2013**, 5, 12.
- [20] S. H. Lee, X. G. Zhang, C. M. Parish, H. N. Lee, D. B. Smith, Y. N. He, J. Xu, *Adv. Mater.* **2011**, 23, 4381.
- [21] K. X. Z. Wang, Z. F. Yu, V. Liu, Y. Cui, S. H. Fan, *Nano Lett.* **2012**, 12, 1616.
- [22] J. A. Huang, Y. Q. Zhao, X. J. Zhang, L. B. Luo, Y. K. Liu, J. A. Zapien, C. Surya, S. T. Lee, *Appl. Phys. Lett.* **2011**, 98, 183108.
- [23] M. Dejarld, J. C. Shin, W. Chern, D. Chanda, K. Balasundaram, J. A. Rogers, X. L. Li, *Nano Lett.* **2011**, 11, 5259.
- [24] L. B. Luo, J. S. Jie, W. F. Zhang, Z. B. He, J. X. Wang, G. D. Yuan, W. J. Zhang, L. C. M. Wu, S. T. Lee, *Appl. Phys. Lett.* **2009**, 94, 193101.
- [25] B. Nie, L. B. Luo, C. Xie, P. Lv, J. S. Jie, M. Feng, F. Z. Li, C. Y. Wu, L. Wang, Y. Q. Yu, S. H. Yu, *Small* **2013**, 9, 2872.
- [26] X. Miao, S. Tongay, M. K. Petterson, K. Berke, A. G. Rinzler, B. R. Appleton, A. F. Hebard, *Nano Lett.* **2012**, 12, 2745.
- [27] Y. L. Cao, Z. T. Liu, L. M. Chen, Y. B. Tang, L. B. Luo, J. S. Jie, W. J. Zhang, S. T. Lee, C. S. Lee, *Opt. Exp.* **2011**, 19, 6100.
- [28] J. M. Liu, *Photonic devices*, Cambridge University Press, Cambridge, **2005**.
- [29] L. J. Yang, S. Wang, Q. S. Zeng, Z. Y. Zhang, L. M. Peng, *Small* **2013**, 9, 1225.
- [30] A. D. Stiff, S. Krishna, P. Bhattacharya, S. W. Kennerly, *IEEE J. Quantum Elect.* **2001**, 37, 1412.
- [31] X. Xie, S. Y. Kwok, Z. Z. Lu, Y. K. Liu, Y. L. Cao, L. B. Luo, J. A. Zapien, I. Bello, C. S. Lee, S. T. Lee, W. J. Zhang, *Nanoscale* **2012**, 4, 2914.
- [32] Y. Jiang, W. J. Zhang, J. S. Jie, X. M. Meng, X. Fan, S. T. Lee, *Adv. Funct. Mater.* **2007**, 17, 1795.
- [33] X. W. Fu, Z. M. Liao, Y. B. Zhou, H. C. Wu, Y. Q. Bie, J. Xu, D. P. Yu, *Appl. Phys. Lett.* **2012**, 100, 223114.
- [34] L. Y. Cao, B. Nabet, J. E. Spanier, *Phys. Rev. Lett.* **2006**, 96, 157402.
- [35] P. W. Barber, R. K. Chang, *Optical effects associated with small particles*, World Scientific, Singapore **1988**.
- [36] M. Schnell, P. Alonso-Gonzalez, L. Arzubia, F. Casanova, L. E. Hueso, A. Chuvilin, R. Hillenbrand, *Nat. Photonics* **2011**, 5, 283.
- [37] B. Desiatov, I. Goykhman, U. Levy, *Nano Lett.* **2009**, 9, 3381.
- [38] E. D. Palik, *Handbook of Optical-Constants*, *J. Opt. Soc. Am. A* **1984**
- [39] W. Gao, J. Shu, C. Y. Qiu, Q. F. Xu, *ACS Nano* **2012**, 6, 7806.